

DEEP DISPOSAL OF SPENT NUCLEAR FUEL

ROLAND PUSCH¹, JÖRN KASBOHM², THAO HOANG-MINH³,
LAN NGUYEN-THANH⁴ & LAURENCE WARR²

¹Luleå University of Technology, Sweden

²Greifswald University, Germany

³VNU University of Science, Vietnam National University, Vietnam

⁴Technical University of Darmstadt, Germany

ABSTRACT

An alternative but still untested approach is to dispose of highly radioactive waste in very deep boreholes, a concept being considered in the UK and the US. One version of this concept known as Very-Deep-Hole (VDH) storage proposes drilling of up to 4 km deep holes and placing in a series of stacked super-containers sealed by a combination of dense clay and concrete. In this case the risk of losing clay material by dispersion and erosion where the holes intersect fracture zones would be eliminated by casting concrete of a new type. VDH containment relies on the use of copper or Navy Bronze tubes filled with dense clay in the upper parts of the holes and with clay-embedded canisters with waste in the lower parts. The maturation and isolating function of the clay seals in the holes and their chemical interaction with concrete and waste canisters are considered and assessed. The work has focused on the mechanical testing and microscope investigations of the clay/concrete. Hydrothermally treated clay and concrete, exposed to 20–150°C, which represents the conditions over the entire length of a real VDH, have been tested. The recorded impact of strong heating showed stiffening and some reduction in hydraulic conductivity of the clay and concrete.

Keywords: nuclear fuel, deep boreholes, clay, concrete, waste disposal, waste isolation, engineered barriers, longevity.

1 INTRODUCTION

The disposal of highly radioactive spent reactor fuel is currently a key issue among the countries using nuclear power. Several disposal concepts have been proposed internationally but major difficulties identified are: 1) the selection of a suitable location of the repositories, 2) the choice of repository design with special respect to the geohydrological and geochemical function of the host rock, 3) the choice of required engineered barriers, 4) the prediction of possibly released radionuclides from waste packages for assessing the effectiveness of waste-isolation. Currently, mined repositories at <500 m are considered to be prime choice, such as the Swedish KBS-3 method, which is presently being evaluated by the Swedish Environmental Protection Agency. Alternative concepts such as disposal in deep boreholes are examined by the UK and US but have not yet been tested [1].

This paper provides an overview of a method for sealing Very-Deep-Holes (“VDH”) in crystalline rock using 2.5 to 4 km deep bored holes with 0.6–0.8 m diameter. In such a scenario the upper half of a borehole can be sealed with dense, expandable clay blocks, whereas the lower half contains clay-lined waste canisters with spent reactor fuel [2]. The role and function of the clays used to seal the holes and to isolate the canisters with waste is dealt with in the paper. They must provide adequate isolation of the holes for tens of thousands of years under temperatures of up to 70°C in their upper parts and 150°C at the base of the lower (“deployment”) parts. If this fails, the safety of the VDH method would rely on the stagnancy of the heavy salt groundwater in the deployment zone. It is unlikely to rise to near surface crustal levels [1].



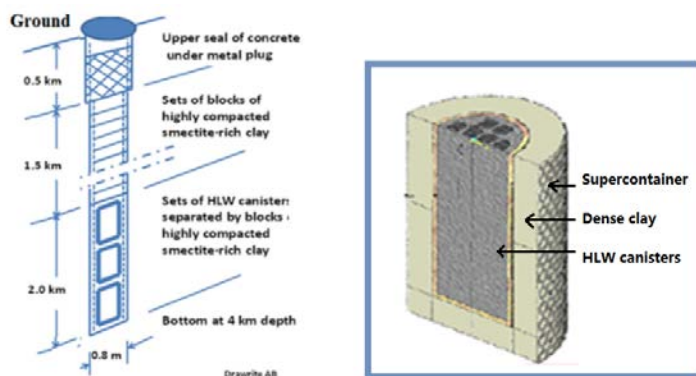


Figure 1: VDH concept for disposal of spent reactor fuel. Left: 4 km deep borehole with 0.6–0.8 m diameter; Right: Clay-lined canister lined in perforated super-container [2], [3].

2 CONCEPT FOR DEEP GEOLOGIC DISPOSAL OF SPENT NUCLEAR FUEL

The described concept for disposal of spent reactor fuel in 2.5 to 4 km deep holes with 0.6 to 0.8 m diameter in crystalline rock, has the waste encapsulated in cupric waste canisters (copper or Navy Bronze). A particularly suitable location of a VDH repository is where interception of groundwater flow is at minimum and structural stability of the host rock is high [2].

Fig. 1 shows a VDH hole that is clay-sealed below an upper surface-near concrete plug, and that hosts waste containers in its lower part. The clay-sealed part, extending from about 0.5 to 2 km depth, overlies the “deployment part”, with canisters of copper or Navy Bronze with 90% Cu, lined with very dense clay. The clay seals and clay-lined canisters are confined in “super-containers” that are perforated for providing the clay components with water required for hydration and swelling. The clay-sealed zone with no waste will experience moderate constant heat (60–70°C) whereas the clay liners and blocks in the deployment zone may be heated up to 150°C for a few hundred years.

3 SMECTITIC ENGINEERED BARRIERS

3.1 Criteria and predicted sealing function

The clay components, which are chemically compatible with the rock and super-containers, will interact and together provide sufficient isolation of possibly released radionuclides by being less permeable than the surrounding rock and by establishing tight contact with the rock. The role of the clay mud in which the super-containers are submerged, is to smear the super-containers when inserted in the holes, and to add to the density of the clay system.

3.2 Constitution of smectitic clay

The dense clay in the super-containers in the upper, sealed zone is the major engineered barrier to prevent water-transported radionuclides to escape up through the holes. The dry density should be high and the hydraulic conductivity, after taking up calcium from the salt-rich groundwater in the rock at more than 1 km depth, be equal to or lower than that of

the surrounding rock [3]. The absence of hydraulic gradients in the host rock makes the clay practically impermeable for any period of time. Clay materials of interest are commercial smectitic clays like MX-80 of Cretaceous age (American Colloid Co), and Holmehus clay of Tertiary age (Dantonite AS), [4]. They are prepared by milling and treatment with sodium carbonate for bringing Na ions into the interlamellar space in order to get favourable geotechnical properties (Tables 1 and 2). Table 3 gives the chemical element composition.

The detailed microstructure of the clay components is illustrated in Fig. 2 for the case of saturated clay components in VDH. “Na soft” represents the initial state of the clay mud and “Na dense” relates to the dense clay core in the super-containers. “Ca soft to dense” represents consolidated smectite clay at depth in VDH.

3.3 Evolution of the clay mud

Freshly-bored deep holes become filled with groundwater with a salinity that increases with the depth. This water shall be replaced by electrolyte-poor tap water that is pumped in from below and is in turn replaced by smectite mud for creating a suitable medium for submerging the super-containers. The bulk density of the mud should be the same as of montmorillonitic drilling muds for making it suitably viscous. The mud stiffens early by thixotropic strength regain and reaches, for a dry density of 160 kg/m^3 , a shear strength of about 1200 Pa in the first few hours. As we will show in the paper the mud will then be integrated with clay migrating out from the super-containers and be denser with time. After one day the hydraulic conductivity of the mud has dropped to about $E-10 \text{ m/s}$, which is

Table 1: Hydraulic conductivity K of Holmehus and MX-80 clays [2].

Densities (kg/m^3)		K , Holmehus (m/s)		K , MX-80 (m/s)	
Saturated density	Dry density	Distilled water	3.5% CaCl_2 solution	Distilled water	3.5% CaCl_2 solution
2000	1590	2E-12	E-11	E-13	5E-13
1850	1350	E-11	5E-11	E-12	5E-12
1570	902	E-10	5E-10	2E-11	5E-11

Table 2: Swelling pressure p_s of Holmehus and MX-80 clays [2].

Densities (kg/m^3)		p_s of Holmehus (MPa)		p_s of MX-80 (MPa)	
Saturated density	Dry density	Distilled water	3.5% CaCl_2 solution	Distilled water	3.5% CaCl_2 solution
2000	1590	2.4	1.5	5.0	4.0
1850	1350	1.3	0.6	1.5	1.0
1570	902	0.3	0.0	0.3	0.0(5)

Table 3: Element data of bulk samples of Holmehus and MX-80 clays [2].

Element	SiO_2	Al_2O_3	Fe_2O_3	MgO	CaO	Na_2O	K_2O
Holmehus	58.6	15.3	6.5	2.2	0.7	1.4	2.8
MX-80	63.6	19.8	5.0	3.2	3.1	2.8	1.0



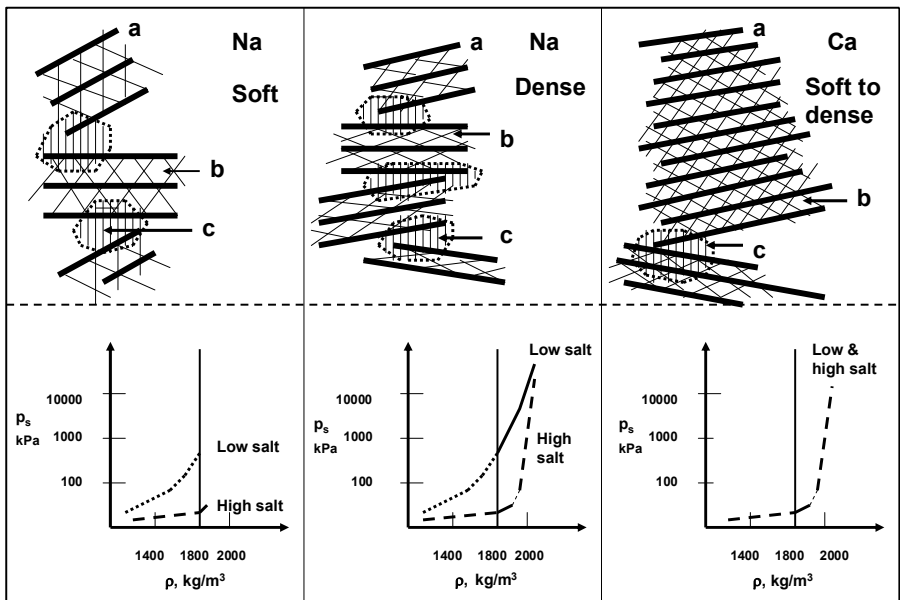


Figure 2: Schematic images of stacks of smectite lamellae and influence of bulk (total) density and porewater salinity on the particle spacing and bulk swelling pressure. (a) Lamella; (b) Interlamellar space; (c) Contact region with interacting electrical double-layers, exposed hydroxyls and polarized adsorbed cations [2], [3].

lower than the conductivity of the surrounding crystalline rock at a few hundred meters depth. Deeper down than 1 km the clay and the rock between the fracture zones have about the same even lower conductivity [2]. The just placed mud forms a largely homogeneous gel that seals the contact between the rock in the holes and the super-containers. Water is sucked from the mud by the very hydrophilic dense clay in the super-containers, which thickens the mud in the course of the expansion.

3.4 Evolution of the clay system in and around super-containers

Fig. 3 illustrates three stages from left to right, i.e. from the prepared units consisting of a central, perforated bronze tube with tightly fitting clay blocks or clay-lined waste canisters (left), followed by submerged units in a mud-filled deposition hole (central), and the fully matured, largely homogeneous system of integrated mud and dense clay (right). The supercanisters can be coated with a thin paste of mixed smectite and talc for delaying hydration of the clay components if required. This is remotely made by robot technique.

3.5 Preparation of holes with mud and dense clay in VDH

The initially very high hydration potential of the dense clay drops with increasing water content and reaches the same value as for the mud if expansion to the same dry density can take place. The dry density of the interacting elements of mud and dense clay in Fig. 4, and

for any pair of adjacent elements within the dense clay, can be predicted by calculating the transport of water from wetter to less wet elements, taking the difference in hydration potential as the driving force. The time for the associated flow to take place is controlled by the transient hydraulic conductivity of the elements (cf. Table 1) [2], [5].

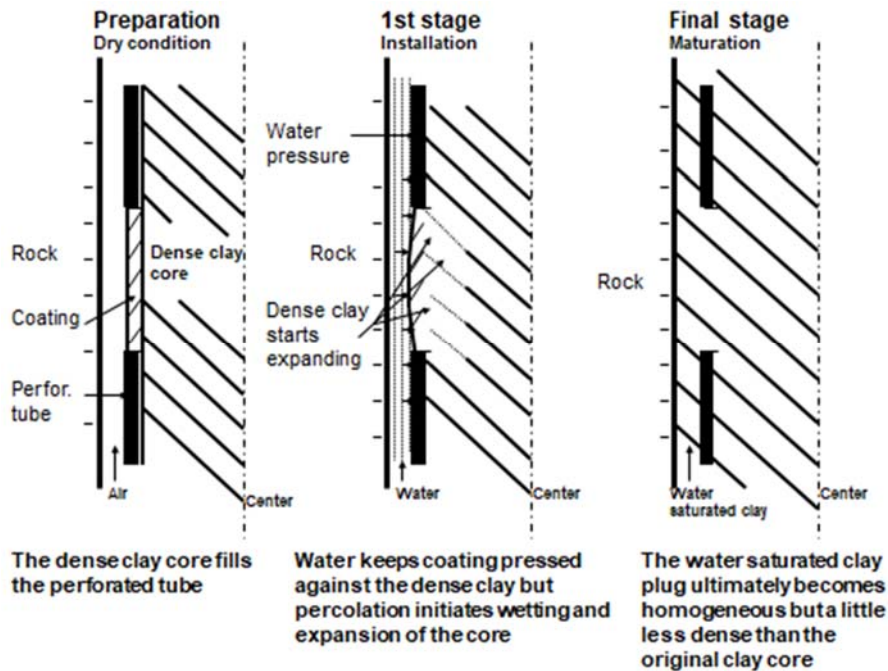


Figure 3: Three stages in the evolution of a sealed VDH.

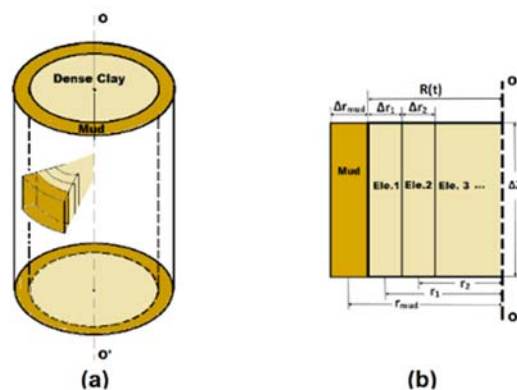


Figure 4: Schematic of specimen. (a) Dense clay core, surrounded by clay mud, absorbs water from the mud in radial direction; (b) Elements for numerical calculation [5].

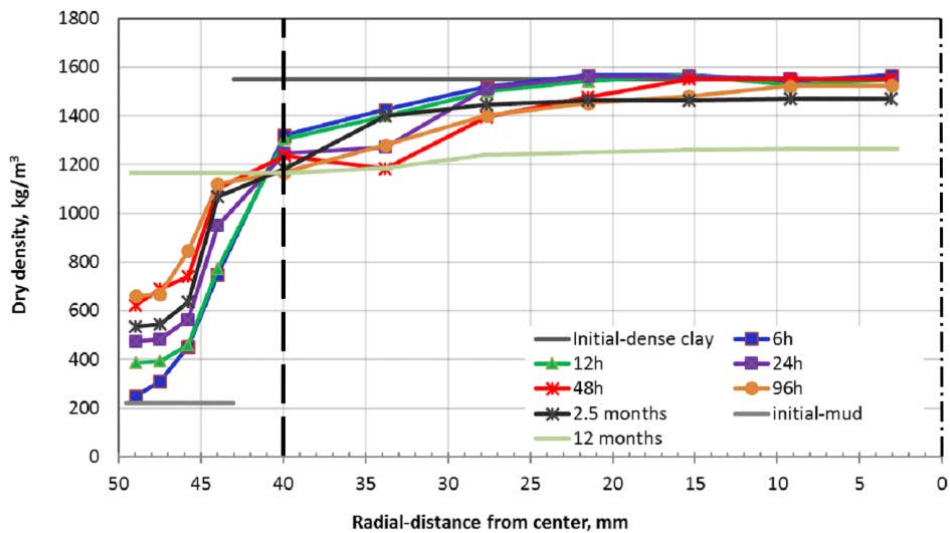


Figure 5: Predicted and recorded densification of mud surrounding a perforated super-container (fat broken line) with the vertical symmetry axis at “0” [5].

Yang (2017) conducted tests on physical VDH models and compared the results with numerical calculations of the type mentioned [5]. The diagram in Fig. 5 gives the results from testing a model with 100 mm diameter of a tube with 50% perforation degree and 10 mm radial space between the tube and a confining cell. It shows that most of the evolution of the mud/clay system took place in a few days but that almost one year was needed to complete the “skin” evolution.

Such tests showed that the clay skin surrounding the perforated tube was less dense at the outer periphery – representing the rock contact – than at the tube wall in the first few days. This demonstrates that the resistance to slip of a super-container, being submerged, is lowest at the rock wall. Assuming similar geometries for a real VDH the average dry density of the skin would shortly be at least 900 kg/m^3 and the hydraulic conductivity would be about $E-10 \text{ m/s}$. The swelling pressure of the clay on the rock would be a few hundred kPa. In the model test the average dry density had risen to 1000 kg/m^3 in a couple of weeks and the average hydraulic conductivity of the skin had dropped to about $5E-11 \text{ m/s}$ whereas the swelling pressure had increased to about 1 MPa. In a real VDH with the same degree of tube perforation, i.e. 50%, and with 10 mm diameter of the perforation holes and 10 mm gap between container and rock, the initial rate of densification will be practically the same as for the model but the larger volume of dense clay will lead to a higher ultimate dry density of the integrated system than for the model. However, homogenization, taking 1 year for the model, will be several decades in a real case since the water flow paths will be longer.

Fig. 6 shows the homogeneity and toughness of the “skin” formed by clay migrated from the dense clay in a super-container.

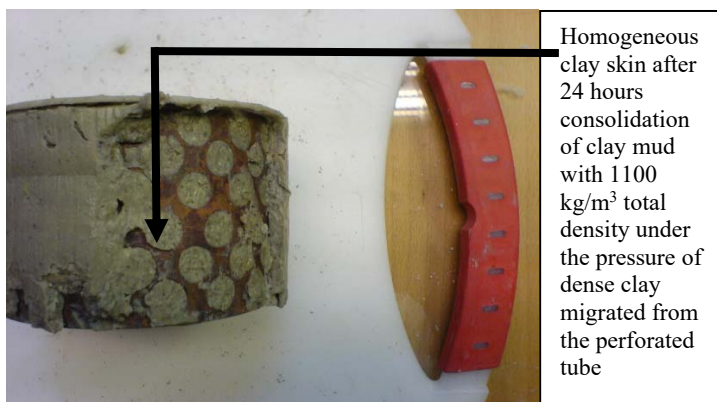


Figure 6: A 2 days old model super-container with 80 mm diameter cell after partial removal of the clay skin emanated from the dense clay with an initial dry density of 1750 kg/m^3 [3].

3.6 Placement and evolution of the engineered barriers

According to the VDH concept, the super-containers are suitably coupled to form two or more units that will sink down to rest on previously placed super-containers under their own weight or be forced down by use of a drill rig [3], [5].

The ultimate saturated density of the integrated mud/block in all parts of a VDH will be about 1900 kg/m^3 , assuming that the initial (dry) density of the blocks are 2050 kg/m^3 , which is achieved by compressing very dry smectite granules under 100–200 MPa pressure [6], [7]. The hydraulic conductivity, which will be about $5\text{E-}12 \text{ m/s}$ according to Table 1 for montmorillonite-rich clay, is lower than the conductivity of the surrounding rock represented by the 20 mm boring-disturbed zone “EDZ” [3]. The density is high enough to make it impossible for microbes to multiply and migrate in the clay [3]. If and where the boreholes have been significantly widened by rock fall, concrete plugs need to be cast [2]. Mixing the mud with very finely ground quartz powder can be made for retarding or preventing mud to move out into rock fractures and be lost [3].

In the present study our reference material MX-80 was saturated with 10% CaCl_2 solution for testing the hydraulic conductivity, ductility and coherence under the arrangement shown in Fig. 5 before and after hydrothermal treatment. The initial dry density of the dense central core was 1590 kg/m^3 while it was 160 kg/m^3 of the surrounding mud. The hydraulic conductivity of the clay was $K=\text{E-}10 \text{ m/s}$ before and after the 3 days long hydrothermal treatment at 95°C . Fig. 7 shows variations in the degree of homogeneity of the microstructure of the hydrothermally treated clay. In Fig. 7 (Left) one can see the coagulated microstructure of the initially soft mud and in Fig. 7 (Right) a couple of shear bands oblique to the macroscopic (straight, white/grey) shear plane of a small shear box.

4 STABILITY OF CLAY COMPONENTS IN VDH

4.1 General

We will deal here with the impact of heat and permeation as well as mechanical strain on the microstructural constitution of the clay embedding the waste canisters in them. Also,



Figure 7: Optical micrograph of hydrothermally treated saturated clay (200X). Left: salt-coagulated microstructure of the initially soft mud; Right: shear zones oriented “west/northwest” in the upper right, and “north/south” in the center. The white spots are CaCl_2 salt precipitates in voids.

we will consider the long-term chemical stability of these clays, which is fundamental to the waste isolation capacity in both short and long term perspectives.

4.2 Hydrodynamic effects

In practice, the hydrostatic pressure in VDH is almost totally determined by the depth below the ground surface where the regional hydraulic gradients are insignificant. The latter can be achieved by locating the deep holes in coastal areas with low topography. Since all technical operations in the holes are performed under water the use of fully pre-saturated clay blocks does not generate hydraulic gradients within them. In contrast, if the clay blocks are not saturated from the start there will be rapid intrusion of water and mud into the blocks via microstructural channels. This is especially so when the clay blocks are placed in the deeper parts of the holes, due to compression of the air-filled voids. Fig. 8 shows that exposure of unsaturated smectite clay to the very high water pressure that is commonly made for determining the hydraulic conductivity, can undergo dramatic microstructural changes. As long as the content of expandable clay particles is high the self-sealing potential of dense smectitic clay is very high.

4.2.1 Mechanical strain and strain rate

A major issue is the mechanical behaviour of the canisters in the super-containers since significant sinking of the canisters due to consolidation or shrinkage of the clay in the latter can create discontinuities and local voids. One reason for this can be creep of the clay that can be predicted by using modern stochastic mechanics based on thermodynamics [8]. Assuming that each transition of slip units, i.e. interparticle bonds, gives the same contribution to the bulk strain, one obtains the expression for the bulk shear strain rate in eqn (1) for shear stresses that are low enough to leave the microstructure intact:

$$d\gamma/dt = B(1 - t/t_0), \quad (1)$$

with the appropriate constant B and the value of t_0 depending on the shear stress, temperature and structural details of the slip process. This gives eqn (2) for the creep for

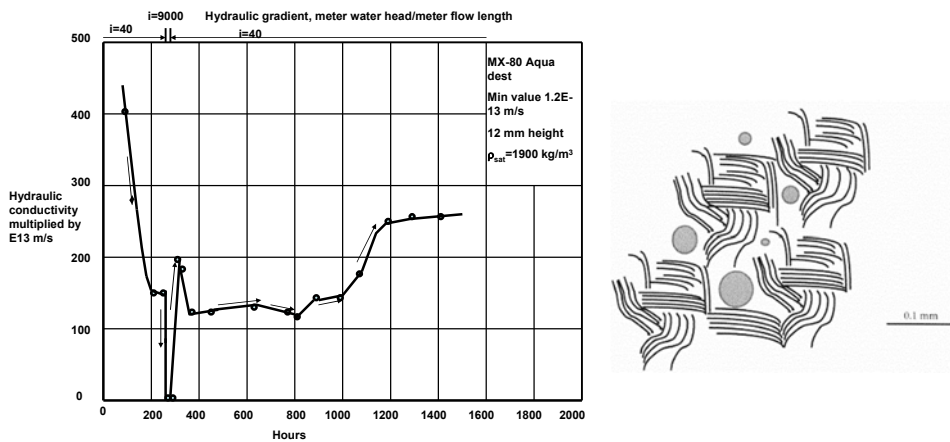


Figure 8: Effect of varying the hydraulic gradient. Until 250 hours the gradient was 40 m/m. From 250 to 255 hours it was 9000 m/m, and then again 40 m/m [6]. Right: Microstructural model of hydrated clay with a bulk total density of 1800–2000 kg/m³ (Dry density 1270–1590 kg/m³).

$t < t_o$ as boundary condition meaning that the creep starts off linearly with time and then dies out. This corresponds to primary creep

$$\gamma = \alpha t - \beta t^2, \quad (t < a/2\beta). \quad (2)$$

For higher bulk loads irreversible changes take place in the form of local microstructural breakdown and reorganization. This mobilizes inflow of new low-energy barriers that increases the number of slips, which are successively being stopped by meeting higher energy barriers. This type of primary creep can go on continuously without bulk failure.

Following Pusch and Feltham [8], thermodynamically defined limits of the energy barrier spectrum are where the strain rate is related to logarithmic creep, taking the form of eqn (3):

$$d\gamma/dt = BT\tau/(t+t_o), \quad (3)$$

where B is a function of the shear stress, and t_o a constant of integration. This leads to a creep relation closely representing the commonly observed logarithmic type, implying that the creep strain is proportional to $\log(t+t_o)$. The significance of t_o is realized by considering that in the course of applying a shear stress at the onset of the creep test, this stress rises from zero to its nominal, final value.

Figs 9 and 10 illustrate shear creep strain of the reference clay MX-80 under relevant, undrained, conditions, showing that the strain rate is low and tends to stagnate for bulk shear stresses lower than about 1/3 of the shear strength determined by traditional methods (triaxial tests, unconfined compression etc). For bulk shear stresses exceeding about 2/3 of the shear strength the strain rate tends to be constant for the initial “primary” and “secondary” creep stages, the latter of which inevitably leads to shear failure.

The case of canister movement within a super-container has been investigated in detail by considering the clay to behave as an elasto/viscous material and using the numerical calculation method of the Boundary Element technique (Fig. 11), [3]. The diagram shows that the settlement was less than $8\text{ }\mu\text{m}$ after 3 months under a constant load of 80 kg (800 N), and that it was approximately proportional to log time. The maximum shear stress was about 17 kPa. Using basic soil mechanis theory failure would be expected for the case of a shear stress of 23 kPa as seen in Fig. 10.

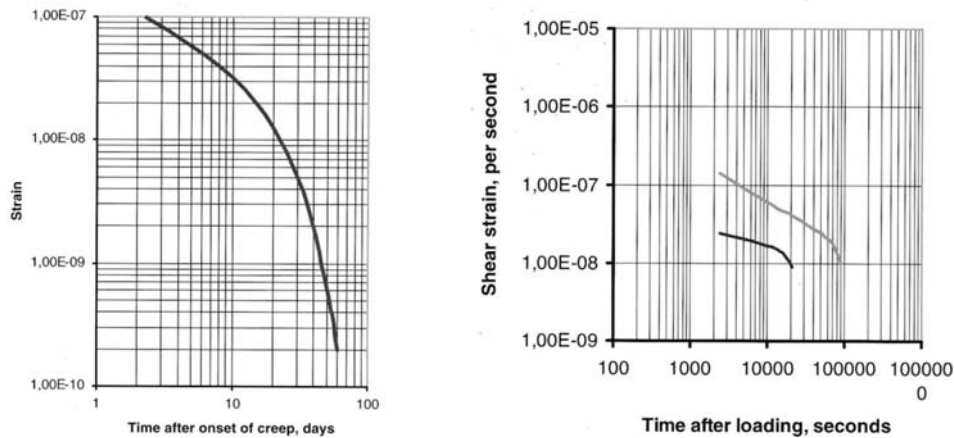


Figure 9: Creep strain rate of smectite-rich clay. Left: Primary creep strain rate of montmorillonite-rich clay with 790 kg/m^3 dry density under a shear stress of 6 kPa; Right: Primary creep of montmorillonite-rich clay with 1490 kg/m^3 dry density under a shear stress of 39 kPa (upper curve) and 23 kPa (lower curve) [3].

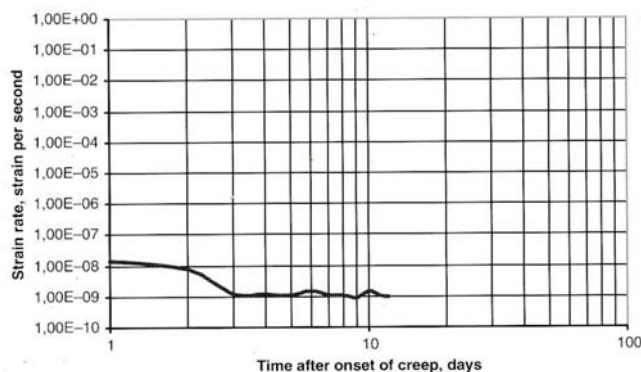


Figure 10: Secondary creep strain rate of montmorillonite-rich clay with 790 kg/m^3 dry density under a shear stress of 23 kPa [3].

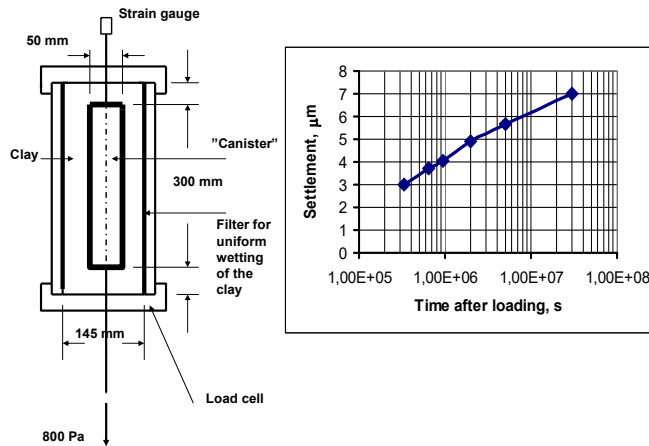


Figure 11: Test with canister exposed to a load of 800 N [3].



Figure 12: Smectite-rich clay migrated into a 1 mm wide fracture in granite [4].

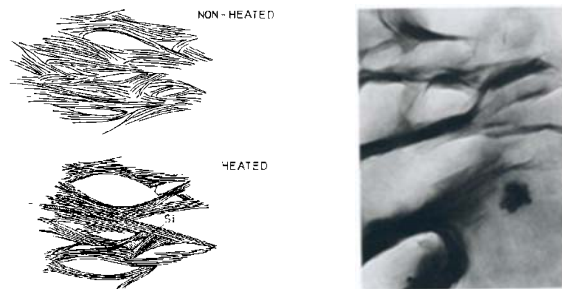


Figure 13: Microstructural change by heating of montmorillonite-rich clay. Left: Coagulation by collapse of interlamellar water structure at $<60^\circ\text{C}$; Right: Mntmorillonite clay with 1590 kg/m^3 dry density, saturated with distilled water, and autoclaved for 6 months. The round objects are Si precipitations (magnification 20000 X), [2].

4.2.2 Rock-sealing ability of clay

The initially soft mud is successively being denser by consolidation under the pressure exerted by the expanding dense clay in the super-containers and is moved into rock fractures and fissures by the swelling pressure of the dense clay (cf. Fig. 12).

4.3 Chemical and mineralogical stability

4.3.1 Impact of heating

We are concerned here with clay blocks made up of aggregates (stacks) of smectite lamellae separated by hydrates and cations. This is akin to the particle interaction model developed by Frenkel for the mutual potential energy per unit area of two interacting semi-infinite particles confining a thin water film [4]. The model shows that such films are not stable at heating and can collapse by which the stacks of lamellae contract as illustrated in Fig. 13, causing an increase in void size but also growth of the mechanical strength.

4.3.2 Mineralogical transformations in the clay seals and practical consequences

Alteration of montmorillonite-rich buffer clay has been thoroughly investigated and is sufficiently well known for accepting such clay as an effective isolation of canisters in repositories for spent fuel, and for sealing of VDHs. Chemical degradation of montmorillonite-rich clay follows in principle the reaction in eqn (4) [9]–[11]:



where S is smectite, Fk is K-feldspars, Mi is mica, I is illite, Q is quartz, and Chl is chlorite.

The reaction formula is a generalization and says nothing about the ways in which the conversion to illite takes place and what the conditions for conversion are. Diagenetic formation of illite and interstratified I/S (illite/smectite) can have the form of dissolution of montmorillonite and precipitation of (20 Å) illite particles. A more important parameter that does not appear explicitly in the equation is the availability and concentration of potassium derived from feldspars, micas and even I/S particles. Temperature becomes the major rate-controlling factor and current illitization models indicate that the following degradation rate – expressed as the percentage of remaining montmorillonite – can be expected for the commonly assumed activation energy 27 kcal/mole at 100°C: 98% after 100 years, 90% after 1,000 years, 50% after 10,000 years and 10% after 100,000 years. For the same activation energy and 150°C: 92% after 10 years, 50% after 100 years, 10% after 1,000 years and 0% after 100,000 years. It follows from this that heating to 90°C for 50 years will hardly cause any loss of montmorillonite at all. A more reactive process, identified in studies of the impact of hydrothermal conditions, is precipitation of cementing agents, since it can cause appreciable stiffening and loss of ductility of the clay. Shearing of a stiff VDH by seismic activity or tectonic rock movements by just centimeters could damage super-containers particularly in the upper part of VDHs. However, the risk of disturbance and damage of the isolating potential of the clay is minimized by locating the clay-isolated parts of the holes between intersected fracture zones, which commonly have larger spacing at depth [2].

The evolution of the clay seals in VDH strongly depends on the temperature, especially at the lower end of the deep holes, where the temperature can be up to 150°C in the first 1,000 years, followed by 60–70°C during the rest of the first 100,000 year period. Common geotechnical data for clays with different montmorillonite content and density indicate that the average hydraulic conductivity for a density of 2,100 kg/m³ at saturation and

percolation with Ca-dominated ocean water will increase from about $5\text{E-}13$ to $5\text{E-}11$ m/s if the montmorillonite content has dropped from 70–80% to 10–15% [4]. The expandability and thereby the self-sealing capacity largely disappears. One notices, however, that also the degraded dense clay still has a hydraulic conductivity of the same order of magnitude as the surrounding rock. After cooling and convergence of the VDH the clay may resemble very stiff and impermeable claystone.

The density of the mud/clay mixture will have increased so much in 48 hours that the super-containers would have to be forced down or require coupling to form long, heavy chains. Even higher mud densities would require loading in combination with vibration. The gamma radiation exerted by the spent fuel is not sufficiently intense to cause practically important mineral conversion or microstructural changes but production of gas, like hydrogen, may cause microstructural changes leading to wider and longer channels [3], [12].

The evolution of the placed clay “buffer system” is concluded to be as follows:

1. The high water pressure causes rapid wetting of initially unsaturated canister-embedding clay [6]. Fully water-saturated clay from the start becomes heated and expanded causing high local porewater overpressure and reduced effective (“grain”) pressure and shear resistance of the clay. The overpressure dissipates by water migration in the shallow bore-disturbed surrounding rock.
2. Anaerobic corrosion of the super-containers and canisters is speeded up and causes early stiffening of the clay by exchange of the initial sodium to be calcium and iron, and precipitation of cementing Fe-compounds [9]. Salt will clog channels in the clay and retard or stop percolation of the salt groundwater in the deployment zone.
3. Gamma radiation generates oxygen and hydroxyls. Oxygen speeds up the corrosion of super-containers and canisters while hydroxyls may dissolve the clay. Both can migrate upwards in gaseous form to the clay-sealed part of the VDH where the high swelling pressure of the still montmorillonite-rich clay prevents or retards gas penetration. Such penetration will take place in a peristaltic fashion at a pressure corresponding approximately to the swelling pressure of the clay [3].
4. For the upper, sealed part of VDH with no waste and with a temperature lower than about 70°C , the most influential factor is pH caused by the proximity of concrete. High Ca- and Mg-contents offer a stabilizing effect (“Sleepers”), while low contents of these elements or high Na content speed up the alteration (“Sprinters”). For the lower, waste-bearing part, with a temperature ranging between about 90 and 150°C , the same effect is expected and the speed of alteration is even higher.
5. The generation of free Si according to Eq.4, partly emanating from exchange of silicons in the Si tetrahedron sites by Al or Mg, and partly from dissolved silicate minerals including clay, is believed to cause precipitation of silicious cementing compounds [2]. This is illustrated by Fig. 14, which also shows the stiffening effect of hydrothermal processes. One observes that stepwise loading of montmorillonite-rich samples after several weeks long hydrothermal treatment at more than 100°C resulted in stiffening, especially by heating at more than 100°C .

4.3.3 Chemical evolution of concrete seals in VDH

A presently favoured recipe (Table 4) requires use of low-pH cement with about 6% cement as binder and quartzite/quartz filler as aggregate. Comprehensive experimental study under hydrothermal conditions has been conducted for identifying and quantifying chemical degradation at temperatures up to 150°C . The results show that the pH of such



concrete with a bulk density of about 2,000 kg/m³ is low enough (pH=10) to leave contacting montmorillonite clay largely unaffected.

Talc concrete of this type has been investigated with respect to its strength properties after exposure to hydrothermal conditions at temperatures of up to 150°C for more than 2.5 months. Samples cured at room temperature for 28 days had a compressive strength of 2.6 MPa, and 4.5 MPa after 45 days. At 150°C, the strength was even higher indicating that this type of concrete has a potential of serving acceptably in deep repositories. Fig. 15 shows successive stages in determining the compressive strength. In VDH the load acting on each concrete plug will be caused by the weight of the respective plug and not of the system of super-containers located on top of it because of wall friction and key effects.

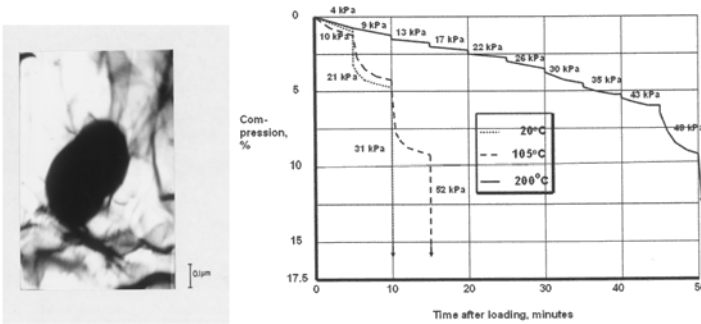


Figure 14: Silica precipitation. Left: Autoclaved Wyoming bentonite with distilled water at 150°C under 20 MPa water pressure. Right: compression of silicified samples with 480 kg/m³ dry density, saturated with distilled water [3].

Table 4: Composition of concrete to be cast in VDH, Weight % [12].

Low-pH cement (Merit 5000)	Talc	Water/cement ratio	Aggregate/cement ratio	Density, kg/m ³	pH
6.5	9.5	3.6	12.8	2070	10

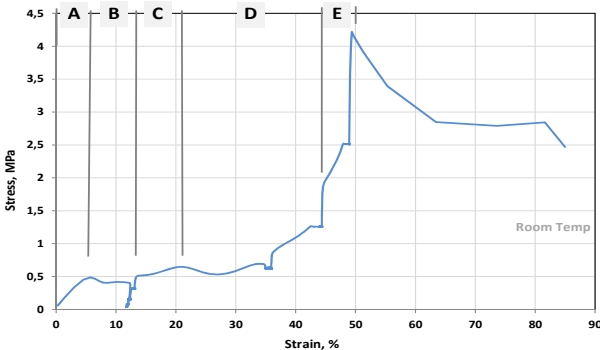


Figure 15: Stress/strain diagram for a compressed clay/concrete sample. A–D= compression to failure of the clay component. E= compression to failure of the concrete [12].

5 CONCLUSIONS AND COMMENTS

The main functional principle of VDH is to prevent possibly released radionuclides from canisters with highly radioactive waste, like spent nuclear fuel, to reach shallow groundwater via the 2.5–4 km deep boreholes. The processes can be summarized as:

Below the uppermost 0.5 km of concrete seals, down to 2.5 km depth [2], [12], [13]:

1. Corrosion of the super-containers will convert them to cupric compounds. Released cations will be absorbed by the clay in the containers, causing cation exchange and slight increase in hydraulic conductivity. This part of a VDH is not expected to leak as the clay will stay ductile and tight for hundreds of thousands of years,
2. Concrete of the proposed type will stay largely intact for very long periods of time because of the low content of cement and the quartz-rich aggregate.

Below the upper clay-sealed zone, from 2.5 to 4 km depth:

3. The high temperature speeds up corrosion which gives high concentration of released elements. However, the high density of the salt-rich water is expected to maintain any contaminated water at least a couple of hundred meters below the parts with no waste,
4. The proposed concrete will have sufficient strength and chemical stability to remain mechanically stable and being low-permeable for very long periods of time.
5. Oxygen and hydrogen will be formed by γ -radiation and significant groundwater convection is expected but the lack of lasting hydraulic gradients means that released radionuclides will migrate by diffusion only, implying that the time for their arrival to the ground surface will be at least 100 000 years.

REFERENCES

- [1] Brady, P.V. et al., Deep Borehole Disposal of High-level Radioactive Waste, SANDIA Report 2009-4401, New Mexico/Livermore California, USA, 2009.
- [2] Pusch, R., Yong, R.N. & Nakano, M., *Disposal of High-level Radioactive Waste*, ISBN 978-0-8153-6766-6; Hard back, Taylor & Francis: New York, 2018.
- [3] Pusch, R., *Geological Storage of Radioactive Waste*, Springer Verlag: Berlin, 2008.
- [4] Pusch, R., *Bentonite Clay. Environmental Properties and Applications*, ISBN-13 978-1-3822-4343-7, Taylor & Francis: New York, 2015.
- [5] Yang, T., Maturation of clay seals in deep boreholes for disposal of radioactive waste. PhD thesis, Luleå Technical University, Luleå, Sweden, 2017.
- [6] Pusch, R. & Yong, R.N., *Microstructure of Smectite Clays and Engineering Performance*, ISBN10: 0-415-36863-4, Taylor & Francis: New York, 2006.
- [7] Svemar, Ch., *Cluster Repository Project (CROP)*, Final Report of European Commission Contract FIR1-CT-2000-20023, Brussels, Belgium, 2005.
- [8] Pusch, R. & Feltham, P., A Stochastic model of the creep of soils. *Géotechnique*, **30**(4), pp. 497–506, 1980. DOI: 10.1680/geot.1980.30.4.497.
- [9] Kasbohm, J., Pusch, R., Nguyen-Thanh L. & Hoang-Minh T., Lab-scale performance of selected expandable clays under HLW repository conditions. *Environmental Earth Sciences*, **69**(8), pp. 2569–2579, 2013. DOI: 10.1007/s12665-012-2085-1.
- [10] Grindrod, P. & Takase, H., Reactive chemical transport within engineered barriers. *Proceedings of the 4th International Conference on the Chemistry and Migration Behaviour of Actinides and Fission Products in the Geosphere*, pp. 773–779, 1994.
- [11] Pytte, A.M. & Reynolds, R.C., The thermal transformation of smectite to illite. *Thermal History of Sedimentary Basins.*, eds N.D. Naeser & T.H. McCulloh, Springer Verlag: Berlin, pp. 133–140, 1989.



- [12] Mohammed, M.H. et al., Interaction of clay and concrete relevant to the deep disposal of high-level radioactive waste. *Applied Clay Science*, **118**, pp. 178–187, 2015. DOI: 10.1016/j.clay.2015.08.008.
- [13] Pusch, R., Warr, L.N., Grathoff, G., Purkbakhtiar, A., Knutsson, S. & Ramqvist, G., A study on cement-poor concrete with talc for borehole sealing in rock hosting radioactive waste. *Comunicações Geológicas*, **100**, pp. 89–98, 2014.

